Possibility of Charge Density Wave Instability in the Barium Tungsten Bronze $Ba_{0.15}WO_3$

Enric Canadell*

Laboratoire de Chimie Théorique (CNRS URA 506), Université de Paris-Sud, 91405 Orsay, France

Myung-Hwan Whangbo*

Department of Chemistry, North Carolina State University, Raleigh, North Carolina 27695-8204

Received July 8, 1993®

The electronic band structure of the $Ba_{0.15}WO_3$ phase was calculated by employing the extended Hückel tight-binding method, and the nature of the partially filled bands was analyzed. $Ba_{0.15}WO_3$ has partially filled bands of one-dimensional (1D) as well as three-dimensional (3D) character. Consequently, $Ba_{0.15}WO_3$ may exhibit a charge density wave (CDW) instability due to the 1D bands but may remain metallic, even after a predicted CDW, because of the 3D band.

Introduction

Barium tungsten bronze Ba_xWO_3 ($0 < x < 0.13$) was first prepared and found to be metallic by Conroy and Yokokawa.[1] Soon Ba_xWO_3 ($x = 0.13$) was reported to become a superconductor at 1.9 K by Sweedler et al.[2] A systematic study of Ba_xWO_3 ($0.01 < x < 0.33$) phases was carried by Ekström and Tilley,[3] who showed that the Ba–W–O system consists of several bronze types, i.e., the tetragonal tungsten bronze (TTB), the orthorhombic intergrowth tungsten bronze (ITB), and $Ba_{0.15}WO_3$. The study of Ekström and Tilley suggests[3] that the $Ba_{0.13}WO_3$ sample prepared by Sweedler et al.[2] is biphasic, containing orthorhombic ITB materials and a larger amount of either the TTB phase or the $Ba_{0.15}WO_3$ phase. From the observations that the TTB phase of the Ba–W–O system is closely related to the tin TTB phase, Sn_xWO_3,[4] which does not become superconducting at least down to 1.3 K,[5] and that only the smaller fraction of Sweedler et al.'s sample (~35%) became superconducting, Ekström and Tilley suggested[3] that the superconducting component of Sweedler et al.'s sample[2] was most likely the orthorhombic ITB part. However, there is no compelling reason why the $Ba_{0.15}WO_3$ phase cannot be a superconducting component. The X-ray crystal structure of $Ba_{0.15}WO_3$ was determined by Michel et al.,[6] who showed that the structure of $Ba_{0.15}WO_3$ is similar to those of $KCuM_3O_9$ (M = Nb, Ta).[7] The electrical resistivity and thermoelectric power measurements for compressed pellets of powder samples and magnetic susceptibility measurements of powder samples show[8] that $Ba_{0.15}WO_3$ is a metal with electron-type carriers. All these physical measurements were carried out down to ~100 K, so that it is unknown whether or not $Ba_{0.15}WO_3$ remains metallic below ~100 K. So far no electronic band structure study has been reported for these barium tungsten bronze systems. In the present work, we calculate the electronic band structure of $Ba_{0.15}WO_3$ on the basis of the extended Hückel tight binding (EHTB) method[9] and analyze the nature of its partially filled bands to examine the anisotropy of the metallic properties. The atomic orbital parameters of our EHTB calculations were taken from our previous study.[10]

Crystal Structure

For our discussion of the electronic band structure of $Ba_{0.15}WO_3$, it is necessary to describe the essential elements of its crystal structure. $Ba_{0.15}WO_3$ is made up of WO_6 octahedra by sharing their corners. A corner-sharing of WO_6 octahedra leads to a WO_5 chain **1**, which can be represented by a top-projection view

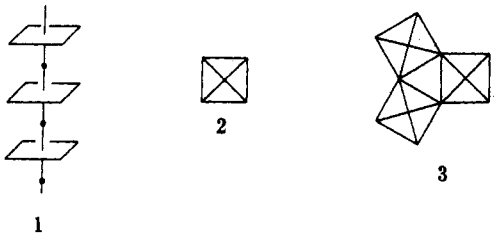

1 **2** **3**

2. The W_3O_{12} chain **3** is obtained when three WO_5 chains share their corners. Alternatively, the W_3O_{12} chain may be considered as constructed from W_3O_{15} cluster units (i.e., the repeat units of the W_3O_{12} chain capped with three oxygen atoms, which are also represented by the projection view **3**) by sharing their three axial oxygen atoms. As shown in **4**, the W_3O_{12} chains share their corners to form the three dimensional (3D) lattice of $Ba_{0.15}WO_3$, which has trigonal, tetragonal and pentagonal channels parallel to the crystallographic c-axis. The Ba^{2+} ions reside in the pentagonal tunnels of **4**.

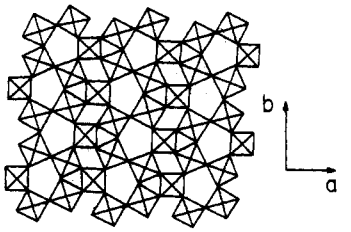

4

In the crystal structure, the W_3O_{12} chains are distorted as shown in **5**. The $W(2)O_6$ and $W(2')O_6$ octahedra have the same geometry, being related by the mirror plane of symmetry that

® Abstract published in *Advance ACS Abstracts*, April 1, 1994.

(1) Conroy, L. E.; Yokokawa, T. *Inorg. Chem.* **1965**, *4*, 994.
(2) Sweedler, A. R.; Hulm, J. K.; Matthias, B. T.; Geballe, T. H. *Phys. Lett.* **1965**, *19*, 82.
(3) Ekström, T.; Tilley, R. J. D. *J. Solid State Chem.* **1979**, *28*, 259.
(4) McColm, I. J.; Steadman, R.; Dimbylow, C. *J. Solid State Chem.* **1975**, *14*, 185.
(5) Gier, T. E. Pease, D. C.; Sleight, A. W.; Bither, T. A. *Inorg. Chem.* **1968**, *7*, 1646.
(6) Michel, C.; Hervieu, M.; Tilley, R. J. D.; Raveau, B. *J. Solid State Chem.* **1984**, *52*, 281.
(7) Groult, D.; Hervieu, M.; Raveau, B. *J. Solid State Chem.* **1984**, *53*, 184.
(8) Michel, C.; Raveau, B. *C. R. Acad. Sci. Paris. Ser. II* **1984**, *299*, 295.
(9) Whangbo, M.-H.; Hoffmann, R. *J. Am. Chem. Soc.* **1978**, *100*, 6093.
(10) Canadell, E.; Whangbo, M.-H. *Phys. Rev. B* **1991**, *43*, 1983.

0020-1669/94/1333-1864$04.50/0

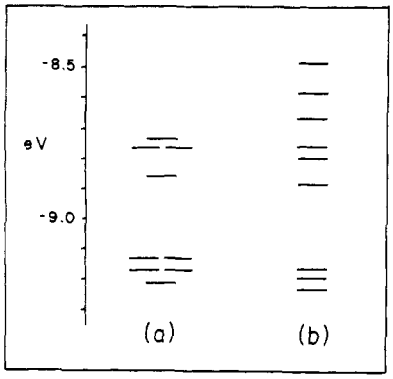

Figure 1. Comparison of the t_{2g}-block levels calculated for (a) the ideal W_3O_{15} cluster and (b) the real W_3O_{15} cluster.

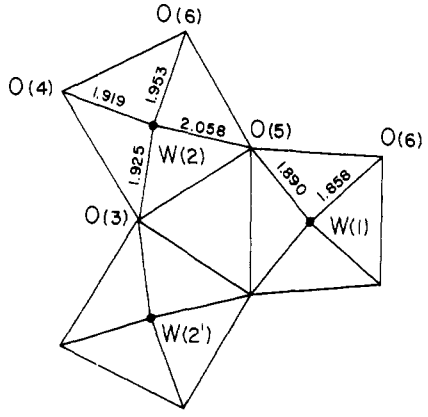

5

bisects the W(1)O6 octahedron. The W(1)–O(6) bonds (1.86 Å) are short compared with other W–O bonds, and the O(5)–W(1)–O(6), O(6)–W(1)–O(6), O(3)–W(2)–O(5), and O(5)–W(2)–O(6) angles are smaller than 90°. Apart from these, the WO_6 octahedra are reasonably regular in shape. In particular, there is no strong W–O···W bond length alternation (1.904, 1.931 Å) along the W_3O_{12} chain direction. In condensing the W_3O_{12} chains to form the 3D lattice **4**, the $W(1)O_6$ octahedra share the O(6) atoms with the $W(2)O_6$ and $W(2')O_6$ octahedra, while the $W(2)O_6$ octahedra share the O(4) atoms with the $W(2')O_6$ octahedra. These structural features play a crucial role in determining the nature of the bottom portion of the d-block bands, as discussed below.

Low-Lying t_{2g} Levels of the W_3O_{15} Cluster Unit

With the typical oxidation states of O^{2-} and Ba^{2+}, there are 0.3 electron per tungsten atom in the d-block bands of $Ba_{0.15}WO_3$, so that only the bottom portions of its t_{2g}-block bands are filled. Since the transport properties of a metal are primarily determined by its partially filled bands, we focus on the bottom portion of the t_{2g}-block bands. The characteristic building blocks of $Ba_{0.15}WO_3$ are the W_3O_{12} chains. Since these chains are made up of the W_3O_{15} cluster units, we first examine the t_{2g}-block levels of the W_3O_{15} cluster.

Figure 1a shows the nine t_{2g}-block levels calculated for the idea W_3O_{15} cluster. (Here the ideal W_3O_{15} cluster was constructed from regular WO_6 octahedra of W-O = 1.93 Å, which is the average of the W-O lengths in **5**.) The bottom five levels of the ideal cluster are described by the orbitals **6a–e**. Along the chain direction, the orbitals **6a–c** make π-type interactions, and the orbitals **6d,e** make δ-type interactions. Figure 1b shows the nine t_{2g}-block levels calculated for the real W_3O_{15} cluster. Due to the distortion **3** → **5**, the real W_3O_{15} cluster has only three t_{2g}-levels as low in energy as the bottom five t_{2g}-levels of the ideal cluster. The most significant change of the distortion **3** → **5** is the W(1)–O(6) bond shortening (see **5**), which raises the level **6d** and leaves

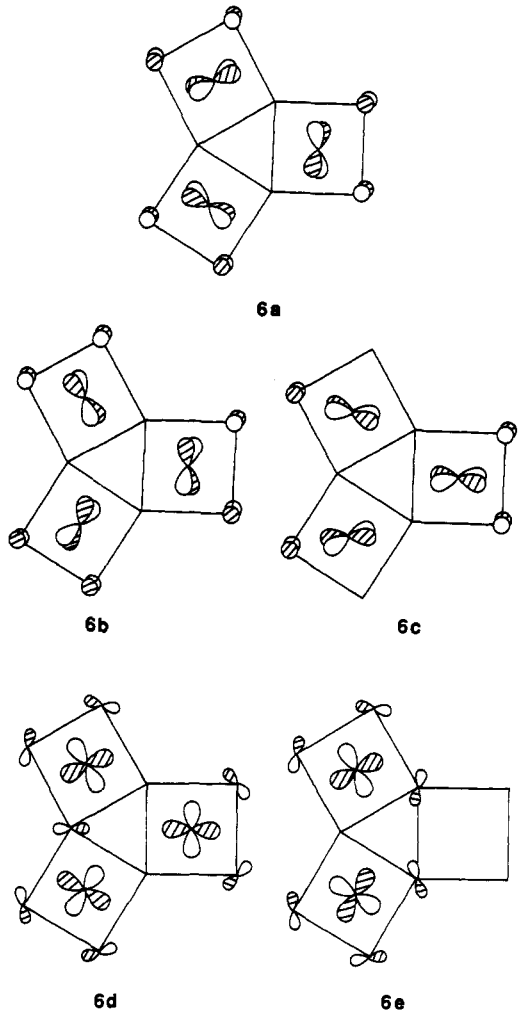

the level **6e** unchanged. The bottom three π-orbitals **6a–c** of the ideal W_3O_{15} cluster rehybridize due to the distortion **3** → **5**, thereby leaving only two π-orbitals (**7a** and **7b**) in the energy

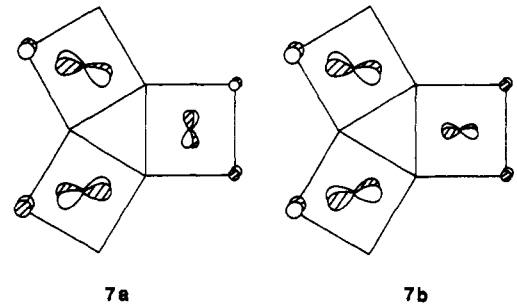

region of **6e**. An important consequence of the distortion is that the orbital contribution of the W(1) atom is made much smaller in **7a,b** than in **6a–c**, thereby reducing the extent of antibonding in the shortened W(1)–O(6) bonds.

Electronic Band Structure

W_3O_{12} Chain. The bottom portions of the t_{2g}-block bands calculated for the ideal W_3O_{12} chains are shown in Figure 2a, where the bands indicated by a star are doubly degenerate. For comparison, the bottom five t_{2g}-block levels of the ideal W_3O_{15} cluster are shown on the right-hand side of Figure 2a. The bands derived from the π-orbitals of the W_3O_{15} clusters are very dispersive, because the absence of W–O···W bond alternation along the chain direction provides strong π-interactions (see **8** and **9**).[11,12] The bands derived from the δ-orbitals of the W_3O_{15}

(11) Whangbo, M.-H.; Canadell, E. *Acc. Chem. Res.* **1989**, *22*, 375.

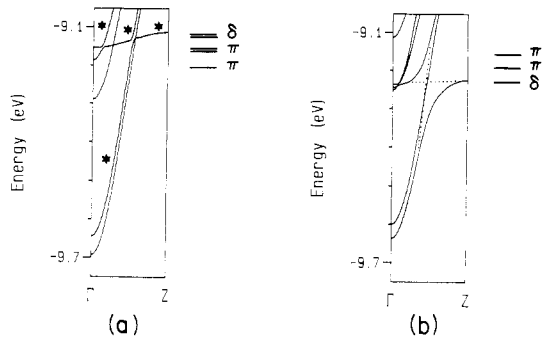

Figure 2. Comparison of the bottom portions of the t_{2g}-block bands calculated for (a) the ideal W_3O_{12} chain and (b) the real W_3O_{12} chain. The bands labeled by a star are doubly degenerate. $\Gamma = 0$ and $Z = c^*/2$.

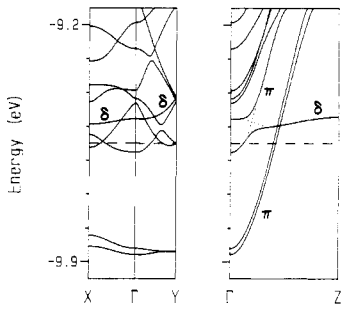

Figure 3. Bottom portion of the t_{2g}-block bands calculated for the WO_3 lattice of the $Ba_{0.15}WO_3$ phase. The dashed line represents the Fermi level. $\Gamma = (0, 0, 0)$, $X = (a^*/2, 0, 0)$, $Y = (0, b^*/2, 0)$ and $Z = (0, 0, c^*/2)$.

clusters are nearly dispersionless because the bridging oxygen orbitals cannot mix with the d orbitals of adjacent W atoms (see **10**).[11,12] Because of the strong dispersion, the bottom of the lowest several π-bands lies well below the δ-bands.

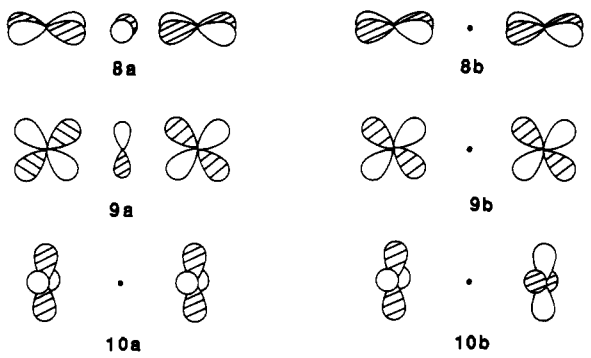

Figure 2b shows the bottom portion of the t_{2g}-block bands calculated for the real W_3O_{12} chain. The three energy levels on the right hand side of Figure 2b represent the bottom three t_{2g}-block levels of the real W_3O_{15} cluster. Analysis of the orbital character reveals that the bottom three bands of Figure 2b are essentially derived from the bottom three d-block levels of the real W_3O_{15} cluster, i.e., **6e**, **7a**, and **7b**. Of these three, one π-band and one δ-band strongly mix and switch their orbital character on going from Γ to Z, as indicated by dotted lines in Figure 2b. The bottom of the two π-bands represent the lowest portion of the t_{2g}-block bands.

WO_3 Lattice. Figure 3 shows the bottom portion of the t_{2g}-block bands calculated for the WO_3 lattice of $Ba_{0.15}WO_3$. In essence, the bottom three bands of the 3D lattice **4** (compare Figures 2b and 3, $\Gamma \rightarrow Z$) are similar in nature to those of real W_3O_{12} chain (Figure 2b); namely, they consist of two π band and one δ band. Since the repeat unit of $Ba_{0.15}WO_3$ is $(Ba_{0.15}WO_3)_6$, there are 1.8 electrons to put into these bands. The dashed line represents the Fermi level coresponding to this electron counting, and this level cuts the two partially filled bands that are strongly dispersive along the chain direction and nearly flat along the directions perpendicular to the chain direction. Another band cut by the Fermi level is dispersive along the three orthogonal directions. Consequently, $Ba_{0.15}WO_3$ possesses partially filled bands of both one-dimensional (1D) and 3D character. The presence of the 1D bands suggests that $Ba_{0.15}WO_3$ is likely to exhibit an electronic instability such as a charge density wave (CDW).[12,13] However, even if $Ba_{0.15}WO_3$ undergoes a CDW transition, as predicted, it may still remain metallic due to the 3D band and may even become a superconductor at a low temperature.

Orbital Character of the Partially Filled Bands. It is of interest to examine why the bottom three bands of the 3D lattice **4** (Figure 3, $\Gamma \rightarrow Z$) are similar in nature to those of the real W_3O_{12} chain (Figure 2b) and also why the two π bands of the 3D lattice are 1D in character. The condensation of the W_3O_{12} chains to form the 3D lattice **4** produces the W–O(6)–W and W–O(4)–W bridges in the directions perpendicular to the chain direction. The 3D lattice **4** can be built in terms of the unit cell **11a**, in which two

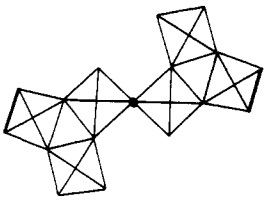

11a

W_3O_{12} chains are condensed by a W–O(4)–W bridge. (For the purpose of clarity, the O(6)–O(6) side of each $W(1)O_6$ octahedron is represented by a thick line in **11a**). When this unit cell is repeated along the b-direction, one obtains a zigzag pattern of W_3O_{12} chains (**11b**) that are joined only by the W–O(4)–W

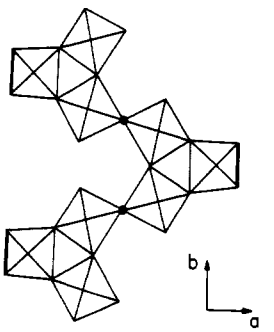

11b

bridges. When the zigzag pattern **11b** is repeated along the a-direction, there occur only the W–O(6)–W bridges between them.

As illustrated in **8**–**10**, there occur three kinds of orbital interactions through a linear symmetric W–O–W bridge. In the π interactions, the p orbitals of the bridging ligand may or may not interact with the metals depending on the relative phases of the metal orbitals (**8a** vs **8b** and **9a** vs **9b**). As already pointed out, two condensed W_3O_{12} chains in a unit cell **11** of the 3D lattice make a W–O(4)–W bridge. Through this bridge, each of the orbitals **6e**, **7a**, and **7b** makes π-type in-phase and out-of-phase combinations. Therefore, there occur two sets of orbitals, the lower energy set with no orbital contribution from the O(4) atom, and the higher energy set with orbital contribution from

(12) Canadell, E.; Whangbo, M.-H. *Chem. Rev.* **1991**, *91*, 965.

(13) Moret, R.; Pouget, J. P. in *Crystal Chemistry and Properties of Materials with Quasi-One-Dimensional Structures*: Rouxel, J., Ed.; Reidel: Dordrecht, The Netherlands, 1986; p 87.

the O(4) atom. It is the lower energy set that represents the three lowest energy bands of the 3D lattice.

In **7a** and **7b** the d_π orbitals of the W(2) and W(2′) atoms are oriented such that they are nearly δ oribtals with respect to the W(2)–O(6) and W(2′)–O(6) bond axes. Consequently, any of the orbitals **7a** and **7b** cannot interact effectively through the W–O(6)–W bridges, so that all interactions between adjacent zigzag patterns **11b** vanish. This accounts for why the bottom two nearly-degenerate π bands exhibit only a weak dispersion along $\Gamma \rightarrow X$. We now consider why these two bands are flat along $\Gamma \rightarrow Y$. The zigzag pattern **11b** links the W_3O_{12} chains along the *b*-direction, which leads to the W–O(4)–W bridges between the W_3O_{12} chains. In **7a** and **7b**, the d_π orbitals of the W(2) and W(2′) atoms are pseudo-δ orbitals along the *b*-direction. These d_π orbitals make π-type interactions through the W–O(4)–W bridges, so that the band levels with no p-orbital contributions of the bridging ligand O(4) atoms constitute the lowest-lying π bands. The nodal properties of the two lowest-lying π bands at Γ are shown in structure **12a,b**, and those at Y in structure **13a,b**. For the purpose of clarity, the d_π orbitals of

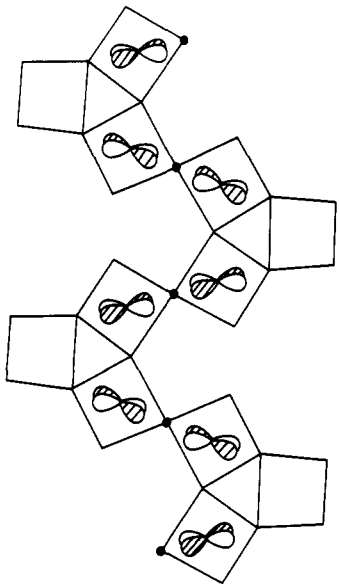

12a

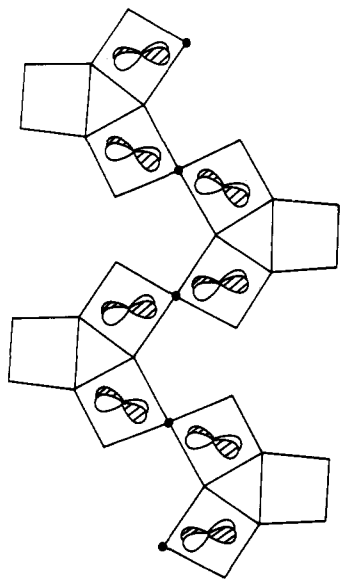

12b

W(1) are not shown in **12** and **13**. At Γ, the band orbital **12a**

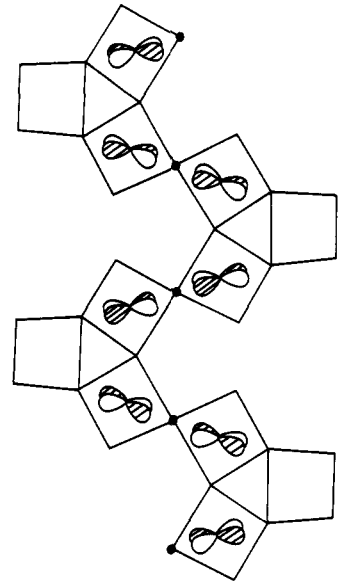

13a

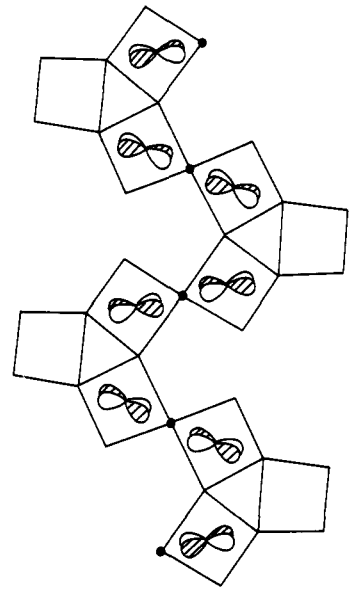

13b

is composed of the cluster orbitals **7a**, while the band orbital **12b** is composed of the cluster orbitals **7b**. At Y, however, each of the band orbitals **13a** and **13b** is constructed by combining the cluster orbitals **7a** and **7b**. (The levels **13a** and **13b** are degenerate as dictated by the glide plane of symmetry present in the zigzag pattern **11b**.) Clearly, in **12** and **13**, the d_π orbitals of the W(2) and W(2′) atoms are pseudo-δ orbitals along the *b*-direction, so that all the levels of **12** and **13** are almost degenerate. This explains why the bottom two π bands are nearly degenerate and are flat along $\Gamma \rightarrow Y$.

In **6e** there is no d-orbital component on the W(1) atom, so that the **6e** do not interact through the W–O(6)–W bridges thereby leading to a flat band in the *a*-direction. Though not shown, the d_δ orbitals of the W(2) and W(2′) atoms of **6e** make π-type interactions through the W–O(4)–W bridges, so that the δ band resulting from the cluster orbitals **6e** are dispersive along $\Gamma \rightarrow Y$ (Figure 3). It should also be noted from Figure 3 that the partially filled band of 3D character in Figure 3 has π character. This band undergoes an avoided crossing with the δ band along $\Gamma \rightarrow Z$ and is dispersive in the directions perpendicular to the chain direction. This band is derived from a W_3O_{15} cluster orbital in which the d_π orbitals of the W(2) and W(2′) atoms make π interactions through the W(2)–O(6) and W(2′)–O(6) bonds, so

that it becomes dispersive along the directions perpendicular to the chain direction.

Concluding Remarks

Our calculations show that the $Ba_{0.15}WO_3$ has both 1D and 3D bands. Due to the 1D bands, $Ba_{0.15}WO_3$ may exhibit a CDW instability. If $Ba_{0.15}WO_3$ undergoes a CDW transition, as predicted, it may still remain metallic due to the 3D band and may even become a superconductor at a low temperature. It is highly desirable to carry out resistivity and X-ray diffraction measurements of single crystal samples of $Ba_{0.15}WO_3$.

Acknowledgment. This work was supported by the U.S. Department of Energy, Office of Basic Sciences, Division of Materials Sciences, under Grant DE-FG05-86ER45259, by NATO, under Grant CRG 910129 from the Scientific Affairs Division, and by Centre National de la Recherche Scientifique, France.